

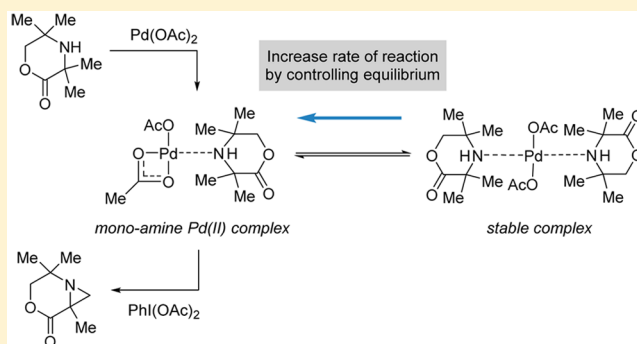
# Mechanistic Insights into the Palladium-Catalyzed Aziridination of Aliphatic Amines by C–H Activation

Adam P. Smalley and Matthew J. Gaunt\*

Department of Chemistry, University of Cambridge, Lensfield Road, Cambridge CB2 1EW, United Kingdom

**S** Supporting Information

**ABSTRACT:** Detailed kinetic studies and computational investigations have been performed to elucidate the mechanism of a palladium-catalyzed C–H activation aziridination. A theoretical rate law has been derived that matches with experimental observations and has led to an improvement in the reaction conditions. Acetic acid was found to be beneficial in controlling the formation of an off-cycle intermediate, allowing a decrease in catalyst loading and improved yields. Density functional theory (DFT) studies were performed to examine the selectivities observed in the reaction. Evidence for electronic-controlled regioselectivity for the cyclopalladation step was obtained by a distortion–interaction analysis, whereas the aziridination product was justified through dissociation of acetic acid from the palladium(IV) intermediate preceding the product-forming reductive elimination step. The understanding of this reaction mechanism under the synthesis conditions should provide valuable assistance in the comprehension and design of palladium-catalyzed reactions on similar systems.



## INTRODUCTION

Transition metal catalyzed activation of aliphatic C–H bonds has emerged as an area of great potential for chemical synthesis through the development of new transformations and the streamlining of complex molecule assembly as well as in the late-stage modification of biologically important entities.<sup>1</sup> Central to the activation of many of these traditionally unreactive C–H bonds is a process called cyclometalation, a functionalization event that steers the metal catalyst to the point of reaction and drives the C–H bond cleavage through proximity; coordination of the metal catalyst to a Lewis basic heteroatom within the directing motif is assumed to lower the entropic and enthalpic costs of the C–H bond cleavage and ring closure.<sup>2</sup> Reaction of the resulting metallocycle with an external species, to form a carbon–carbon or carbon–heteroatom bond, completes the overall functionalization process. Several functionalities can participate in this “directed” C–H activation, such as carbonyl derivatives, aromatic nitrogen heterocycles, and hydroxyl motifs,<sup>3</sup> and arguably, palladium complexes have been most successful at promoting catalytic C–H functionalization in aliphatic systems. As a result, cyclopalladation has underpinned a number of useful catalytic aliphatic C–H bond functionalization processes that have expanded the toolbox of reactions available to synthetic chemists.

Given the palladium-coordinating ability of aliphatic amines, it is surprising that they are seldom used in catalytic C–H activation reactions in comparison to other synthetically important and polar functional groups.<sup>4</sup> However, it is precisely

this strong coordination that limits their utility in C–H activation. When treated with palladium(II) salts, two molecules of the aliphatic amine coordinate to the electrophilic metal center to form coordinately saturated square-planar complexes, a species that is often unreactive to C–H cleavage (Figure 1a).<sup>5</sup> As a result, C–H activation on aliphatic amines requires their derivatization with electron-withdrawing protecting groups or bespoke directing groups in order to achieve a successful reaction, which reduces the overall efficiency of the

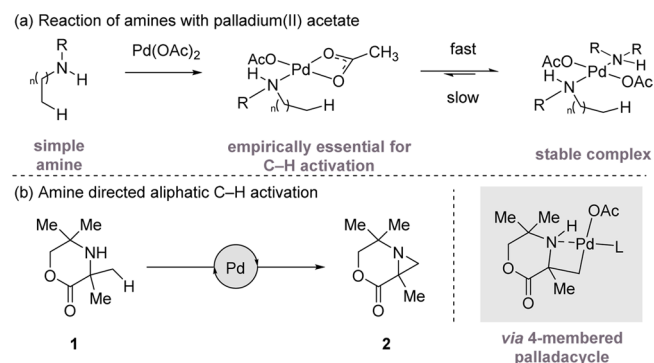


**Figure 1.** (a) Amine coordination to palladium(II) salts results in stable complex formation. (b) System under study in this report: amine-directed aliphatic C–H functionalization.<sup>6</sup>

Received: May 28, 2015

Published: August 6, 2015

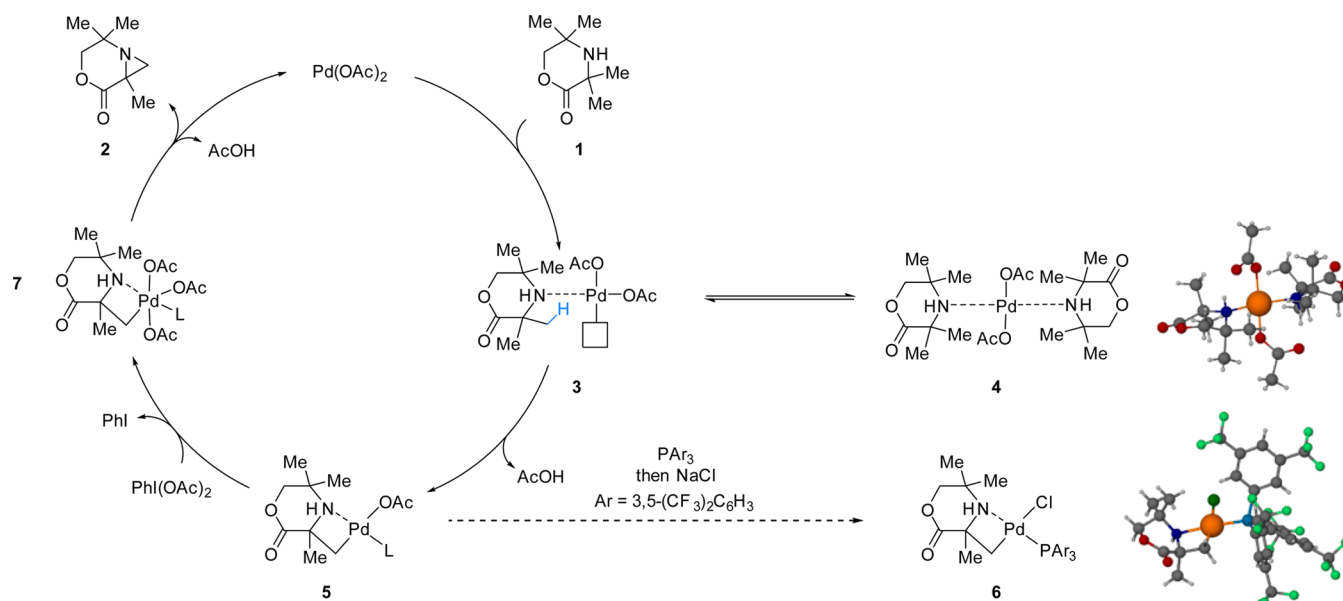


**Figure 2.** Postulated mechanism based on our previous study<sup>6</sup> along with intermediates characterized by X-ray crystallography. Morpholinone **1** coordinates to the metal catalyst but can only undergo C–H activation when there is a vacant coordination site. Palladacycle **5** is presumably oxidized to a palladium(IV) species **7** (L is an undefined neutral ligand), which can then reductively eliminate to give product **2**. Palladacycle **5** was observed through crystallization on addition of a phosphine ligand to give **6**.

C–H transformation. Aliphatic amines are, however, particularly important functional groups because they are common in pharmaceuticals, synthesis building blocks, natural products, and polymeric materials. Therefore, the development of new catalytic C–H activation modes for aliphatic amines is an important challenge for the continual advance of chemical synthesis.

As part of our overarching goal to develop new activation modes for catalytic C–H activation, our group recently reported the use of an unprotected aliphatic secondary amine to direct a palladium-catalyzed C–H functionalization (Figure 1b). This activation mode resulted in the transformation of a methyl group adjacent to the amine motif via a four-membered ring cyclopalladation pathway.<sup>6</sup> In one of the two novel transformations detailed in that initial report, we described a C–H amination to form aziridines. A fully substituted and unsymmetrical secondary amine, morpholinone **1**, underwent C–H activation to form a four-membered ring palladacycle that following the action of a hypervalent iodine oxidant promoted C–N bond formation to aziridine **2**. This aziridination had several interesting features that would have been difficult to predict with the current understanding of C–H activation processes.

Although a comprehensive understanding of this reaction mechanism would allow us to logically move toward further reaction optimization, we also wanted to rationalize (a) why the cyclopalladation occurred with extremely high regioselectivity, even though there appeared to be a choice of sites to react, and (b) why an aziridine was furnished as the final product, unlike the acetoxyated product often obtained under similar conditions.<sup>3a,7</sup>

Herein we report detailed mechanistic studies on the palladium-catalyzed aziridination of tetramethylmorpholinone **1**. Furthermore, density functional theory (DFT) calculations were performed to gain additional insight into the reaction. As a result, we were able to gain a comprehensive understanding of the factors that influence the catalytic C–H activation reaction,

and improvements in the reaction conditions for aziridination were realized.

## RESULTS AND DISCUSSION

At the outset of our studies, we were able to propose a basic reaction mechanism upon which we could formulate more advanced studies (Figure 2). We had previously observed that mixing two equivalents of amine **1** with palladium acetate resulted in isolable bis-amine palladium(II) complex **4**. On warming this complex, we had been able to identify putative C–H activation complex **5**, which following treatment with a phosphine, resulted in mononuclear cyclopalladation species **6**, as determined by X-ray diffraction of a single crystal. The catalytic cycle was believed to conclude with oxidation of the palladacycle by the hypervalent iodine  $\text{PhI}(\text{OAc})_2$ , followed by C–N reductive elimination of resulting palladium(IV) species **7**.

**Kinetic Studies.** Our kinetic protocol features experiments to probe the reagent concentration dependencies and isotopic labeling to interrogate the mechanism of the reaction in Figure 2. The process was monitored by aliquotting the reaction mixture and measuring the concentration by gas chromatography (GC) with 1,1,2,2-tetrachloroethane as an internal standard. The original reaction conditions involved the treatment of amine **1** with 5 mol % palladium acetate, 1.5 equiv of  $\text{PhI}(\text{OAc})_2$ , and 2.0 equiv of acetic anhydride in a solution of toluene stirred at 70 °C. However, in order to simplify the system and remove any extraneous factors that may complicate the analysis, we monitored the reaction with just starting amine, catalyst, oxidant and solvent. This led to a rate profile that appeared to be linear but was only ~30% complete in 500 min (Supporting Information). Doubling the concentration of catalyst to 10 mol % allowed us to follow the whole reaction over an appreciable time scale and revealed that the reaction rate increases during the majority of the reaction (up to ~90% conversion), only leveling off at the very end (Figure 3). Notably, the rate of product formation is roughly equal to

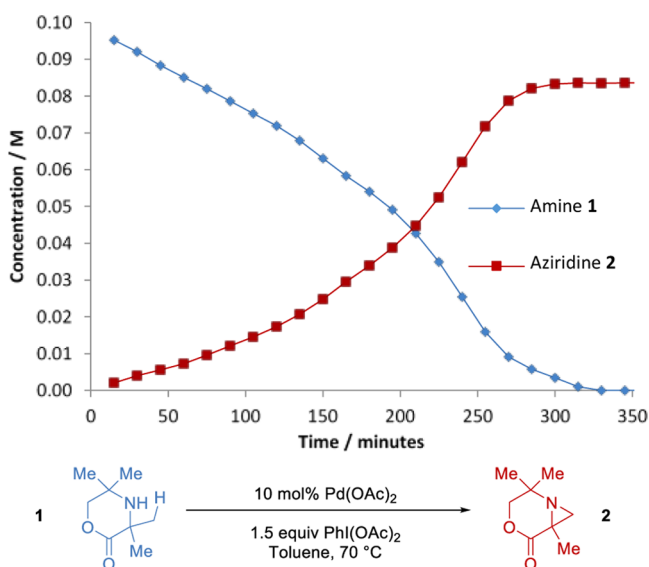


Figure 3. Reaction profile for the above aziridination.

the rate of starting material usage, so our analyses using initial rates are based on starting material concentration so as to minimize any errors in the concentration measurement.

The increase in reaction rate over time suggested to us that there was either a negative-order dependence on amine **1**<sup>8</sup> or that the reaction was autoinductive. The autoinduction could be a result of rate acceleration by the action of product aziridine **2** or by the acetic acid or phenyl iodide byproducts. To test for autoinduction, same “excess” experiments were performed.<sup>9</sup> This analysis is equivalent to carrying out identical reactions at two different starting points and is often used to probe product inhibition and catalysis deactivation. In this case, the reaction was started at 20% completion. If a (by-)product catalyzes the reaction, then the reaction starting at 20% completion will be slower than the reaction that started from 0% completion. Simply overlaying the plots after adjusting the 20% completion reaction for time so that the initial amine concentrations are equivalent shows that there are negligible differences in the rate profiles (Figure 4). We also tested the effect of adding the (by-)products (0.2 equiv of PhI, 0.2 equiv of aziridine **2**, or 0.4 equiv of AcOH) to the 20% completion reaction. In the cases of PhI and aziridine **2**, negligible differences in the rate were observed. However, if we added 0.4 equiv of AcOH to the reaction, then a marginal increase in rate was observed (Supporting Information). Although these results suggested that the result was not autoinductive, we did note the effect of AcOH, and this is discussed in more detail later.

Therefore, we reasoned that the rate increase was due to a negative-order dependency of amine **1**. By comparing the initial rate of reaction with that at 50% conversion, we saw that the rate had doubled suggesting an approximate order of  $-1$  with respect to substrate. However, because the rate decreases at the end, the situation is more complex than this (vide infra).

The order with respect to reaction of the other components in the mixture was then investigated. Because of the linear nature of the kinetic profile at the start of the reaction, the initial rate may be determined from the gradient of the concentration profile during this period. It was found that the reaction is zero-order with respect to  $\text{PhI}(\text{OAc})_2$  suggesting that the turnover limiting step (TOLS) occurs before the oxidation step. Furthermore, the linear variation of rate with

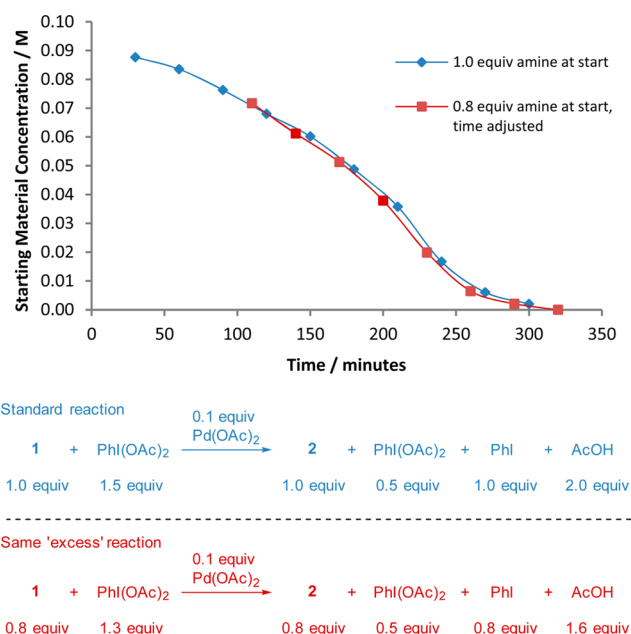


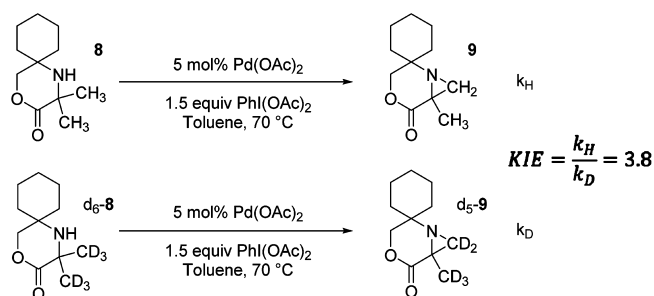
Figure 4. Probing potential autoinduction by carrying out two reactions at the same “excess” but at different initial amine concentrations.<sup>9</sup> The two plots overlap when time-adjusted, suggesting that there is no autoinduction. Reaction conditions for 1.0 equiv amine: amine **1** (0.10 M),  $\text{Pd}(\text{OAc})_2$  (0.01 M),  $\text{PhI}(\text{OAc})_2$  (0.15 M), toluene, 70 °C.

catalyst concentration revealed that the reaction was first-order with respect to  $\text{Pd}(\text{OAc})_2$  (Supporting Information).

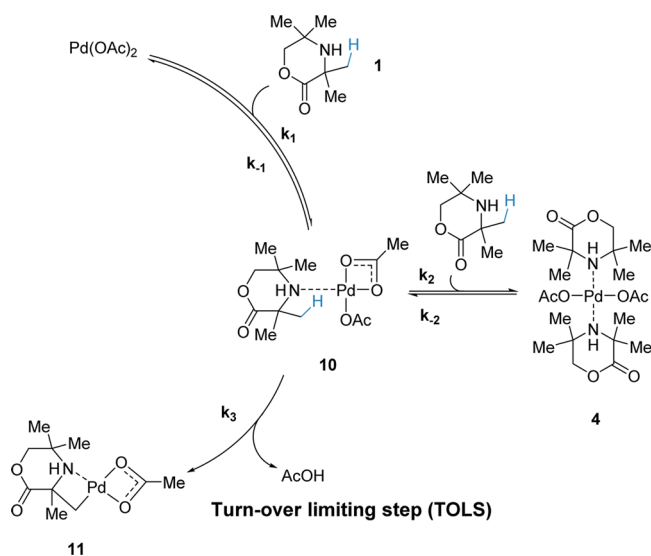
Further kinetic information was obtained by measurement of the kinetic isotope effect (KIE). To prevent any possible regioselectivity issues between the two sets of methyl groups on amine **1** that may interfere with labeling experiments, we opted to test cyclohexane-derivative **8** on the basis of the fact that competing methylene C–H activation would be negligible.<sup>10</sup> After confirming that this substrate was viable in the C–H aziridination, the KIE was determined from initial rate measurements of substrates **8** and  $d_6$ -**8** (Scheme 1). A value of 3.8 was obtained, which is indicative of a primary isotope effect, suggesting that C–H bond cleavage occurs as part of the TOLS.<sup>11</sup>

Consolidation of the mechanism proposed in Figure 2 with the above kinetics data allowed us to provide a set of kinetically important elementary steps with which to test the experimental data (Scheme 2). An equilibrium exists whereby amine **1** can coordinate to the catalyst to give monocoordinated intermediate **10**. This intermediate can then undergo cyclo-

#### Scheme 1. KIE Measured from Comparison of Initial Rates of Amines **8** and $d_6$ -**8**



## Scheme 2. Proposed Elementary Steps in the Kinetically Important Region of the Catalytic Cycle



palladation in the TOLS or coordination with a second molecule of amine **1** to give bis-amine complex **4**. It is proposed that bis-amine complex **4** is an off-cycle intermediate, and previous literature suggests that a vacant coordination site is required for C–H activation to occur via the assumed concerted metalation–deprotonation pathway.<sup>12</sup> We assumed that any isomerization of the acetate ligands to provide the vacant site cis to the amine is expected to be so fast as to be kinetically negligible.<sup>5</sup>

Evidence in support of this bis-amine complex being an off-cycle intermediate was obtained by comparing the reaction profiles of two sterically different amines. It was found that the aziridination of a more hindered amine **12** was faster than that of the tetramethyl amine **1** (Figure 5a). This could be indicative of faster C–H cleavage or an increased concentration of the active monocoordinated species through destabilization of the off-cycle bis-amine complex, on the basis of increased steric interactions between the amine and palladium center. To show that the rate increase was a result of suppressing the formation of this unproductive species, a 1:1 mixture of amines **1** and **12** was subjected to the catalytic conditions. Both species reacted at the same rate to form corresponding aziridines **2** and **13** (Figure 5b). Notably, the rate of formation of **2** in the competition experiment is greater than that observed in isolation. This suggests that the increased rate of reaction for the more hindered substrate (**12**) was not a result of a lower energy C–H activation but instead because of alteration of the mono-/bis-amine equilibrium.

Next, we set up a mathematical description of the reaction in order to allow quantitative agreement of our experimental data and qualitative insights. Because of the observed primary KIE, the rate of reaction is proposed to be given by the C–H activation step itself; this is also consistent with the measurement of oxidant concentration being zero-order. To enable derivation of the rate law, we assumed that all the intermediates following the TOLS provided a negligible contribution to the total catalyst mass. Consideration of the elementary steps in the reaction then led to the theoretical rate law (Scheme 3). This rate law accounts for the initial pseudo-first order of reaction with respect to catalyst measured experimentally; initially, the high substrate concentration can be considered a constant. The

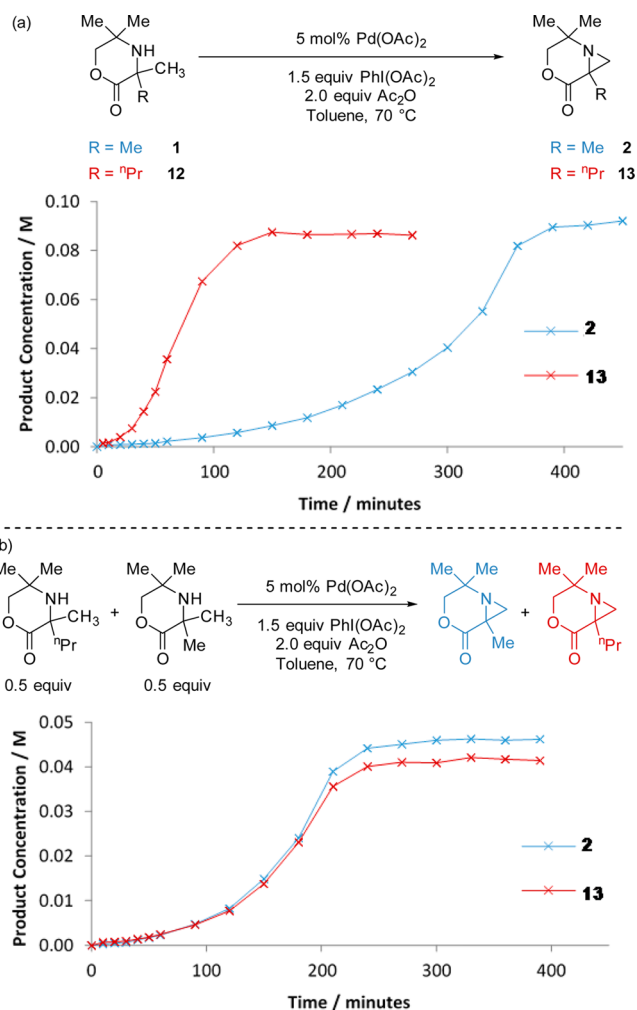


**Figure 5.** (a) Reaction rate of the more hindered amine **12** is faster than that of tetramethyl amine **1**. (b) If these amines are mixed in a 1:1 ratio, then they both react at the same rate.

Scheme 3. Derivation of the Rate Law<sup>a</sup>

On-cycle

$$k_{-1}[\mathbf{10}] = k_1[\text{cat}][\mathbf{1}]$$

Off-cycle

$$k_2[\mathbf{10}][\mathbf{1}] = k_{-2}[\mathbf{4}]$$

Catalyst mass balance

$$[\text{Pd}]_{\text{total}} = [\text{cat}] + [\mathbf{10}] + [\mathbf{4}] = [\mathbf{10}] \left( \frac{k_{-1}}{k_1[\mathbf{1}]} + 1 + \frac{k_2[\mathbf{1}]}{k_{-2}} \right)$$

Rate law

$$\text{Rate} = -\frac{d[\mathbf{1}]}{dt} = \frac{d[\mathbf{11}]}{dt} = k_3[\mathbf{10}] = \frac{k_3[\text{Pd}]_{\text{total}}}{\left( \frac{k_{-1}}{k_1[\mathbf{1}]} + 1 + \frac{k_2[\mathbf{1}]}{k_{-2}} \right)}$$

<sup>a</sup>Cat = Pd(OAc)<sub>2</sub> catalyst; [Pd]<sub>total</sub> = initial concentration of Pd(OAc)<sub>2</sub>.

reaction is also negative first-order with respect to substrate at high substrate concentrations, accounting for the increase in rate over the majority of the reaction, but changes to first-order with respect to substrate at the end, accounting for the “tailing-off” at the end of the reaction.



By assuming that the amine concentration,  $[1]$ , is large, we can take the rate law derived in Scheme 3 and obtain an approximation for the initial rate, eq 1. This assumption is based on the concentration of bis-amine complex 4 dominating  $[10]$  and  $[cat]$ ; this is supported by computational calculations that suggest that the formation of 4 from 10 is favored by 8.43 kcal mol<sup>-1</sup> (Supporting Information).

$$\text{Initial rate} \approx \frac{k_{-2}k_3 [\text{Pd}]_{\text{total}}}{k_2 [1]} \quad (1)$$

Varying the concentration of amine 1 while keeping the catalyst concentration constant allows the determination of  $k_{-2}k_3/k_2$  to be  $0.12 \pm 0.02 \text{ M s}^{-1}$  (Supporting Information). Unfortunately, attempts to directly measure  $k_2/k_{-2}$  by <sup>1</sup>H NMR were unsuccessful because of the overlapping peaks of the metal species; therefore, we were unable to determine a value for the rate constant of C–H activation,  $k_3$ .

**Kinetics-Led Reaction Optimization.** We had previously found that the addition of 0.4 equiv of acetic acid to the reaction mixture had a small but still noteworthy effect on the rate of reaction. On the basis of this, we questioned whether a much higher concentration of acid could lead to a further increase in the rate of reaction. The presence of acid in the reaction mixture should lead to some protonation of the amine and set up an equilibrium between the protonated and free-based amine.<sup>13</sup> If a proportion of the amine is protonated, then it is no longer able to coordinate to the metal, and the effective concentration of free-amine is lowered. As the reaction progresses, the acid equilibrium shifts to provide more free-based amine and effectively delivers a slow release of substrate. By keeping the amine concentration low, less palladium is sequestered in unproductive off-cycle bis-amine complex 4, leading to an increase in the overall rate of reaction. This is conceptually related to an organocatalytic reaction reported by Blackmond where control of an off-cycle species led to rate acceleration.<sup>14</sup>

Hence, increasing the concentration of acid was found to increase the rate of reaction; although at very high acid concentrations, this increase in rate was offset by degradation of the final product (Figure 6). Other acids, such as benzoic acid and pivalic acid, were also found to give rate acceleration. However, because the optimum acid loading was found to be 20 equiv, acetic acid was used because it is cheaper, and as a

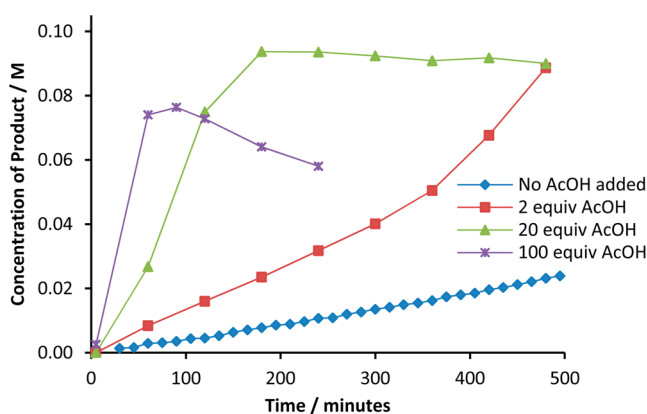


**Figure 6.** Increasing the concentration of acetic acid in the reaction mixture increases the rate of reaction. Reaction conditions: amine 1 (0.10 M), Pd(OAc)<sub>2</sub> (0.005 M), PhI(OAc)<sub>2</sub> (0.15 M), toluene, 70 °C.

liquid, its use is more practical. It is important to note that we have not ruled out the possibility that the acetic acid is hydrogen bonding to amine 1 rather than formally protonating the amine; however, this still provides the desired decrease in free-substrate concentration.

Even though we believed that the beneficial addition of acetic acid was a result of limiting the formation of bis-amine intermediate 4, it is important to consider other possible effects of acetic acid. Previous work by Ryabov<sup>5</sup> on an amine-directed sp<sup>2</sup> C–H activation showed that addition of acid fully protonated the amine and changed the TOLS from C–H activation to dissociation of the Pd(OAc)<sub>2</sub> trimer. The subsequent C–H activation on this multimetal complex was proposed to be faster because of the production of species with vacant coordination sites or more labile acetates. This explanation was unlikely here because even though Pd(OAc)<sub>2</sub> predominantly exists as a trimer in the solid phase and at 37 °C in benzene it has been shown to exist as a monomer at 80 °C in benzene.<sup>15</sup> Nonetheless, this possibility was still ruled out by testing for a KIE with acetic acid present in the reaction. A primary KIE (3.9 vs 3.8 previously) was observed, indicating that the TOLS is still the C–H activation step. From the addition of acetic acid, we also noted that no H incorporation was detected in the deuterated aziridine product, suggesting that the C–H/D activation step is not reversible under these conditions.

We also considered that a Fujiwara-type cationic intermediate may form,<sup>16</sup> whereby the C–H activation onto the putative cationic palladium species is faster, speeding up the reaction.<sup>1a,17</sup> However, from initial observations this was judged to be unlikely because formation of the Fujiwara cationic species with acetic acid has only been reported with sp<sup>2</sup> C–H activations and trifluoroacetate ligands on palladium are required for sp<sup>3</sup> C–H activation via this method.<sup>18</sup> Addition of trifluoroacetic anhydride or trifluoroacetic acid was found to shut the reaction down, whereas using palladium(II) trifluoroacetate instead of Pd(OAc)<sub>2</sub> as the catalyst led to a slower, poor-yielding reaction.

We had previously noted<sup>6</sup> that acetic anhydride was beneficial to the reaction; however, unlike with acetic acid, changing the concentration of acetic anhydride had little effect. We suspect that the main effect of this additive is the removal of water.<sup>19</sup> Water was found to be detrimental to the reaction;<sup>20</sup> furthermore, the removal of water by the anhydride leads to the production of rate accelerating acetic acid.

Taken together, addition of 20 equiv of acetic acid and 2 equiv of acetic anhydride led to an improved reaction, giving an isolated yield of 85% after 2.5 h (Figure 7).

The generality of the newly optimized conditions were tested with a selection of amine substrates (Figure 8). Furthermore, the aziridination of amine 16 proceeded smoothly under the reaction conditions. This conversion of amine 16 to aziridine 17 rules out a general pathway for aziridination that proceeds first via acetoxylation and then displacement to form the three-membered ring. It was found that the reaction worked well using industry-preferred ethyl acetate as the solvent.<sup>21</sup> The catalyst loading could also be lowered, and reaction of amine 1 on a gram scale with 1 mol % Pd(OAc)<sub>2</sub> in ethyl acetate gave an 87% yield of the aziridine product.

**Computational Investigations.** We next performed a series of density functional theory (DFT) studies to gain insights into the regioselectivity of the C–H activation step and the chemoselectivity of the C–N reductive elimination.<sup>22</sup> The

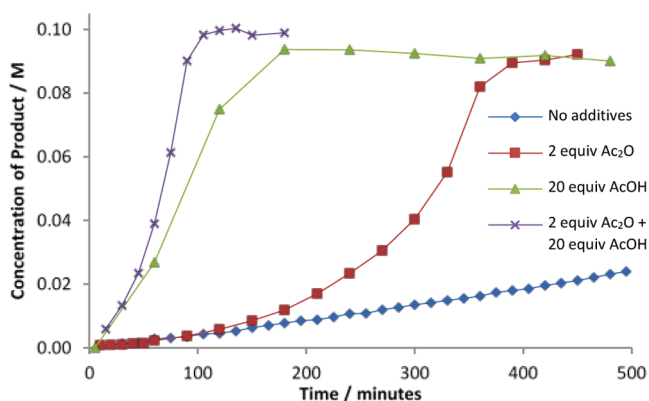


**Figure 7.** Effect of acetic acid and acetic anhydride additives on the reaction profile. Reaction conditions: amine **1** (0.10 M), Pd(OAc)<sub>2</sub> (0.005 M), PhI(OAc)<sub>2</sub> (0.15 M), toluene, 70 °C.

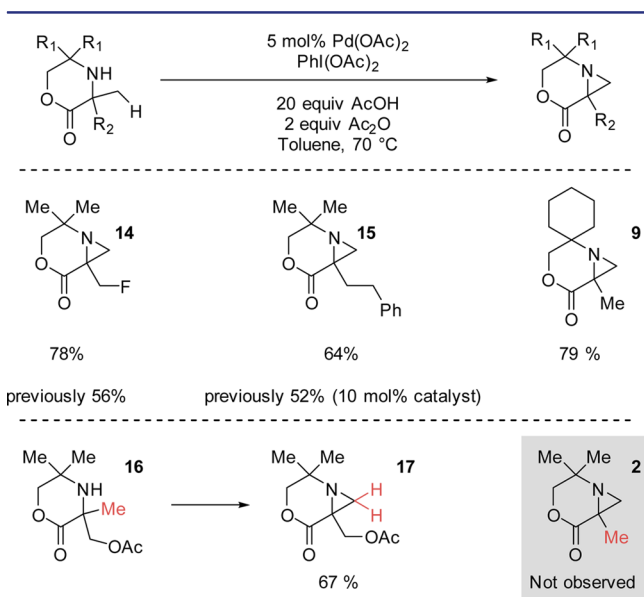


**Figure 8.** Optimized conditions have improved the yield of previous substrates.<sup>6</sup> In addition, amine **16** undergoes aziridination through C–H activation rather than S<sub>N</sub>2-type displacement of acetate under the reaction conditions.

calculations were performed using the Amsterdam Density Functional (ADF) program<sup>23</sup> at the relativistic ZORA-BLYP-D3/TZ2P level of theory, previously benchmarked for palladium catalysis with added dispersion corrections.<sup>24</sup> The inclusion of dispersion corrections has been shown to be important when bulky hydrocarbons are present because interactions that may previously have been considered as repulsive are, in fact, attractive.<sup>25</sup> Solvation by toluene was computed using the COSMO solvation model, and vibrational frequency analysis was performed to confirm that the structures were either minima or transition states.

We first wanted to understand the regioselectivity of the C–H activation step. Initially, the geometry of monocoordinated intermediate **10** was calculated. It was found that there exists a hydrogen bond between one of the acetate ligands on the metal and the N–H of the substrate similar to that seen in the crystal structure of bis-amine complex **4** (Figure 2).<sup>26</sup> The other acetate ligand binds in a  $\kappa^2$  mode so as to maximize bonding interactions. The transition states for C–H activation at the methyl groups on either side of the nitrogen were then

calculated. The cyclopalladation was proposed to occur via monocoordinated intermediate **10** on the basis of the above kinetics data and previous reports indicating the necessity of a vacant coordination site for C–H activation.<sup>5,12a</sup> The unlikelihood of an oxidative addition C–H activation, because of the resulting high-energy palladium(IV) species that often require strong oxidants, and the large primary KIE, suggesting a linear transition state,<sup>10,27</sup> meant that the mode of cyclopalladation was expected to proceed via a concerted metalation–deprotonation (CMD) pathway (Figure 9).<sup>12b,28</sup>

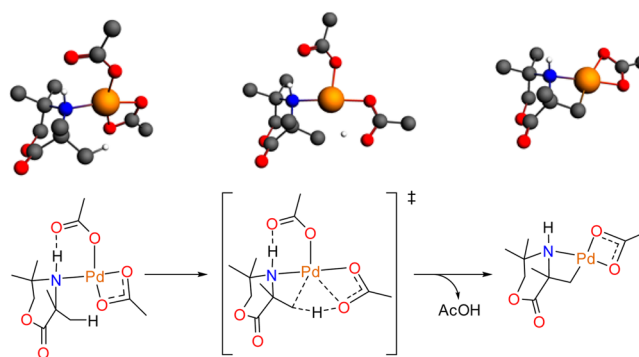


**Figure 9.** C–H activation through a concerted metalation–deprotonation pathway.

Application of this CMD approach on the two possible sites resulted in the transition state for the observed regioselectivity being lower in energy by 4.89 kcal mol<sup>−1</sup> (Figure 10), suggesting that this mechanism is an appropriate representation of the cyclopalladation step.

We speculated that the observed selectivity was either a result of the difference in polarity of the methyl groups, because of differing distances from the carbonyl group, or the change in

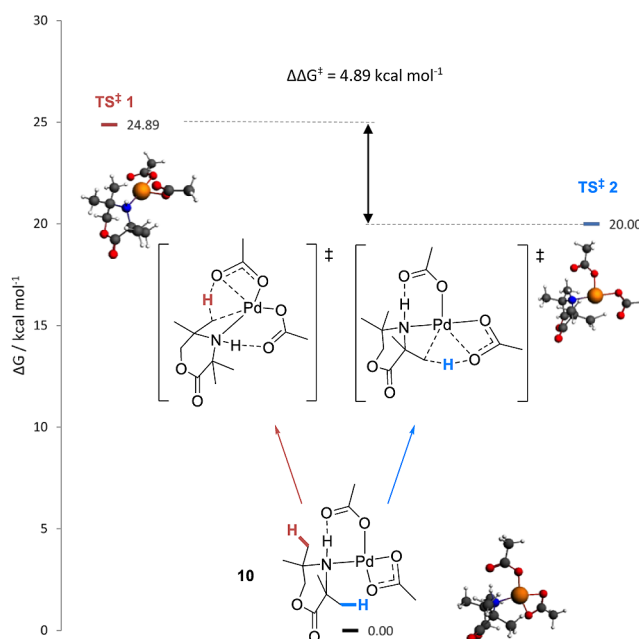


**Figure 10.** As expected from experiment, the transition state for C–H activation at the methyl groups nearest the carbonyl (TS<sup>‡</sup> **2**) is lower in energy than that at the methyl groups furthest from the carbonyl (TS<sup>‡</sup> **1**).

shape of the ring, caused by the ester motif. This question was probed using a distortion–interaction analysis, a method that has been useful in understanding selectivity by splitting the activation energy into a steric component and an electronic component.<sup>29</sup> Fragmentation of the transition state along the new bonds being formed and calculation of the interaction energy between these fragments in the transition state geometry allows us to determine the distortion energy required to position the fragments in the required shape for reaction to occur. By fragmenting as shown in Figure 11 to reform the

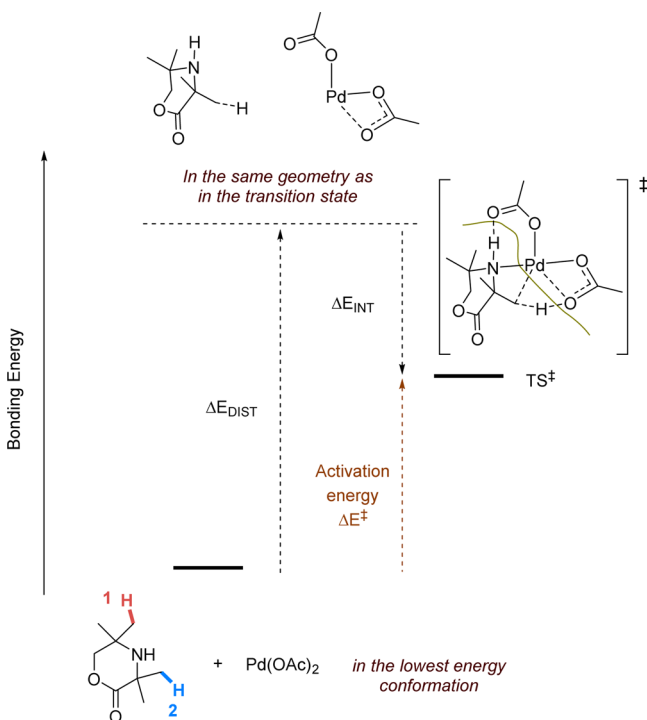


**Figure 11.** Distortion–interaction model splits the activation energy into two components. Fragmenting as shown in the  $\text{TS}^\ddagger$  and calculating the interaction energy between the fragments gives the interaction energy ( $\Delta E_{\text{INT}}$ ). The distortion energy ( $\Delta E_{\text{DIST}}$ ) can subsequently be calculated from knowledge of the activation energy ( $\Delta E^\ddagger$ ).

substrate and  $\text{Pd}(\text{OAc})_2$ , we can see that the disfavored pathway actually has a lower distortion penalty (Table 1). This

**Table 1. Distortion–Interaction Analysis of the Two Possible C–H Activation Pathways<sup>a</sup>**

	$\Delta E^\ddagger$	$\Delta E_{\text{DIST}}$	$\Delta E_{\text{INT}}$
$\text{TS}^\ddagger 1$	2.70	85.12	–82.42
$\text{TS}^\ddagger 2$	0.08	87.97	–87.89

<sup>a</sup>Note that the small values for  $\Delta E^\ddagger$  are as a result of fragmenting back to the substrate and catalyst rather than the (lower energy) monocoordinated intermediate (10). Energies are reported in kcal mol<sup>–1</sup>.

suggests that the flattening of the ring is not responsible for the selectivity. The increased distortion energy for the observed regioselectivity is offset by a greater increase in interaction energy, suggesting that it is the electronic effects of the carbonyl that are important. This can be explained by an increased acidity of the C–H bonds closest to the carbonyl in the ring that lowers the energy required to cleave the C–H bond during

the metal activation step.<sup>30</sup> We believe that this analysis is valid even though we fragment back past the monocoordinated intermediate because both pathways go through the exact same monocoordinated intermediate, 10.

The reaction after the TOLS was proposed to proceed via oxidative addition of the palladacycle with  $\text{PhI}(\text{OAc})_2$  followed by C–N reductive elimination of the resulting palladium(IV) species to provide the product (Figure 2). The use of  $\text{PhI}(\text{OAc})_2$  to access high-valent palladium is well-precedented, with the palladium(IV) species undergoing facile reductive elimination.<sup>2c,31</sup>

However, although reductive elimination from palladium(IV) is well-known, the chemoselectivity of C–heteroatom reductive elimination is poorly understood where multiple competing pathways exist;<sup>32</sup> therefore, any extra insight into this process is of high value. Reaction via a bimetallic palladium(III) intermediate as characterized by Ritter<sup>33</sup> was considered. However, this was deemed to be unlikely here because of the high-energy species formed from the hindered amines stacking on top of each other in the palladium(III) dimer. This supposition was borne out by calculations suggesting that the palladium(IV) intermediate was more favorable.<sup>34</sup>

We initially tested the C–N and C–O reductive elimination pathways directly from proposed palladium(IV) intermediate 18 (Figure 12).<sup>35</sup> Counter to our expectations, C–O bond formation via  $\text{TS}^\ddagger 4$  was a lower energy process than C–N bond formation via  $\text{TS}^\ddagger 3$ .<sup>36</sup> This reaction pathway is therefore not feasible because the resulting acetoxyated product (16) has been experimentally ruled out as an intermediate in the formation of the aziridine (Figure 8). We then considered the possibility of acetic acid dissociation from 18, via  $\text{TS}^\ddagger 5$ , to give complex 20 where the nitrogen atom now formally acts as an anionic ligand. Pleasingly, the C–N reductive elimination via  $\text{TS}^\ddagger 7$  to form the aziridine was now lower in energy than both the competing C–O reductive elimination via  $\text{TS}^\ddagger 6$  and the C–O reductive elimination via  $\text{TS}^\ddagger 4$ . This is consistent with previous work on C–H amination with amide-directing groups;<sup>37</sup> the nitrogen atoms are formally deprotonated in the proposed catalytic cycles and lead to C–N reductive elimination as the major pathway. The possible dissociation of acetic acid from the palladium(IV) intermediate is perhaps not too surprising because the electronegative oxygen atoms in the morpholinone may lead to an increase in acidity of the N–H bond and therefore lower the energy of the deprotonated pathway.

For completeness, we also calculated the pathway for C–N bond formation by  $\text{S}_{\text{N}}2$ -type attack by the uncoordinated amine. We found that even though transition state  $\text{TS}^\ddagger 9$  of the C–N-bond-forming step was comparable in energy with the lowest energy C–N reductive elimination transition state  $\text{TS}^\ddagger 7$  the reactive conformation cannot be reached. In order for the geometry of the palladium(IV) species to be reactive to  $\text{S}_{\text{N}}2$ , the amine must dissociate from the palladium(IV) center (breaking both the amine–palladium bond and the O–H hydrogen bond) and rotate. It was found that the energy required to do this was prohibitively high ( $\text{TS}^\ddagger 8$ ), so we do not believe that the  $\text{S}_{\text{N}}2$  pathway is operable.

As a result of our studies, we are now able to propose a more complete mechanistic picture of this unusual C–H activation reaction (Scheme 4). Amine 1 first coordinates to palladium acetate to give monocoordinated intermediate 10. This species can either coordinate to another amine, to form off-cycle bis-amine intermediate 4, or can undergo the TOLS of

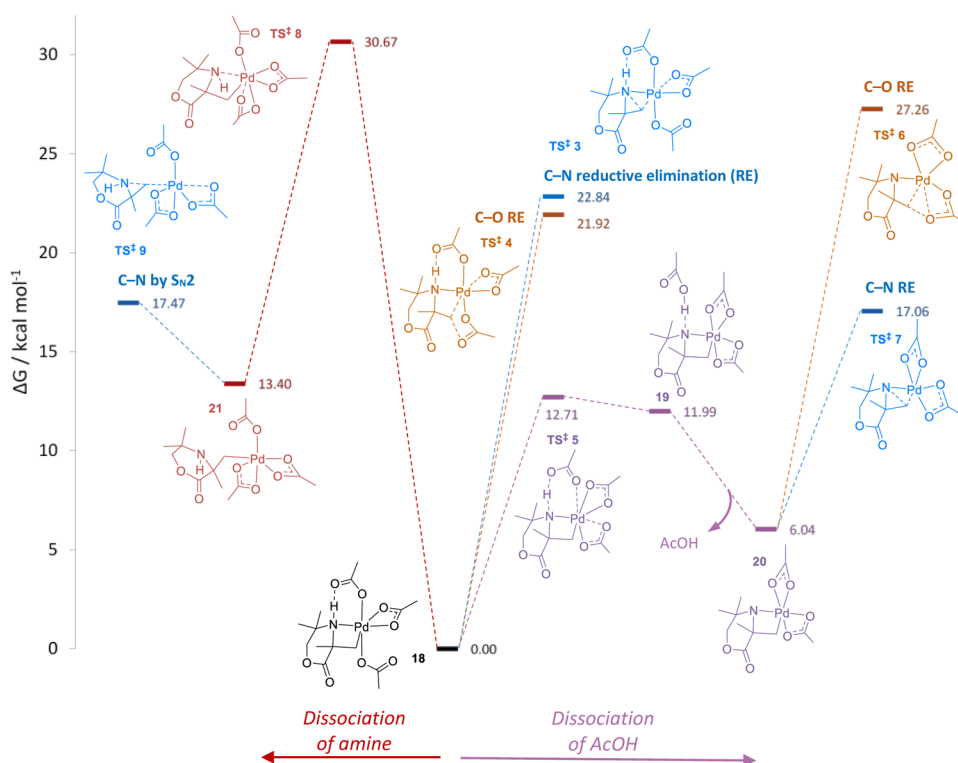
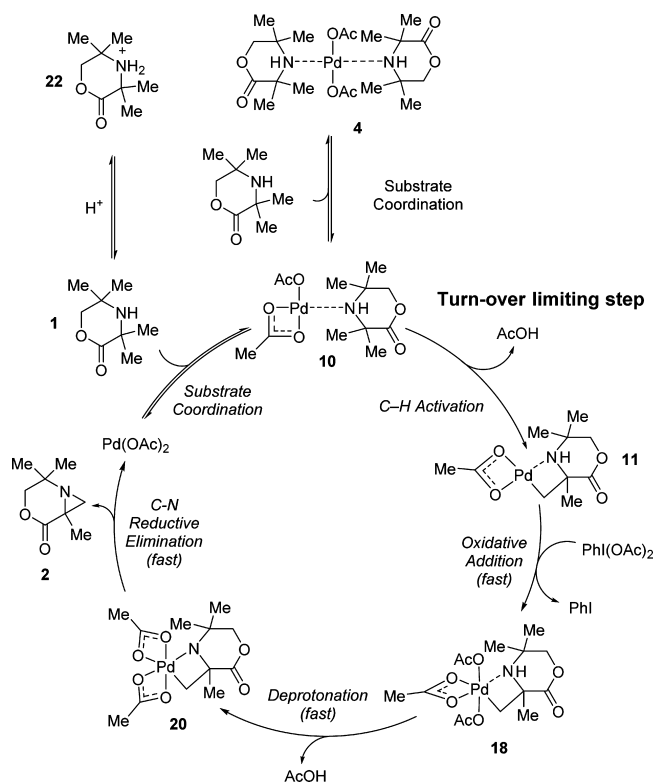


**Figure 12.** Possible pathways to form either a C–O or C–N bond. Reductive elimination from initial palladium(IV) intermediate **18** is a high-energy pathway, and the reaction instead proceeds through rapid deprotonation of the coordinated amine, liberating acetic acid, to give intermediate **20**. Reductive elimination from this species is the lowest energy pathway and favors C–N bond formation (TS<sup>‡</sup> **7**). Even though the transition state for C–N bond formation through S<sub>N</sub>2-type attack of the free amine, TS<sup>‡</sup> **9**, is similar in energy to the reductive elimination through TS<sup>‡</sup> **7**, accessing the necessary conformation is prohibitive because of the high energy barrier (via TS<sup>‡</sup> **8**) associated with the dissociation of the nitrogen atom from the metal center.

#### Scheme 4. Final Catalytic Cycle



intramolecular C–H activation to form a four-membered ring palladacycle **11**. This intermediate is now susceptible to oxidation by  $\text{PhI}(\text{OAc})_2$  and forms palladium(IV) intermediate **18**. Dissociation of acetic acid precedes C–N reductive elimination to provide the aziridine product and also reforms the active catalyst. Furthermore, the overall concentration of amine **1** is modulated by an acid-mediated equilibrium that provides a slow release mechanism for the substrate into the cycle and limits formation of off-cycle bis-amine intermediate **4**.

#### CONCLUSIONS

The mechanism of this novel native amine-directed sp<sup>3</sup> C–H activation has been elucidated by detailed kinetic studies. Suppression of the formation of the off-cycle bis-amine complex by the addition of acetic acid was found to significantly increase the overall rate of reaction. The results of these studies have been used to improve yields of reaction as well as to provide a more synthetically useful procedure that is more applicable for large-scale chemistry. DFT calculations have given an insight into the regioselectivity of cyclopalladation and have provided a plausible explanation for the resulting aziridine product.

We are currently investigating how we can use this understanding to design ligands that can control the C–H activation step with the overall goal of creating an asymmetric process. We hope that these insights into the behavior of palladium(IV) lead to the rational design of related C–H functionalization reactions.



## ■ ASSOCIATED CONTENT

### Supporting Information

The Supporting Information is available free of charge on the ACS Publications website at DOI: 10.1021/jacs.5b05529.

Experimental procedures, characterization data, and computational details. (PDF)

## ■ AUTHOR INFORMATION

### Corresponding Author

\*mjpg32@cam.ac.uk

### Notes

The authors declare no competing financial interest.

## ■ ACKNOWLEDGMENTS

We are grateful to the EPSRC and Pfizer for a studentship (A.P.S.) and the ERC and EPSRC for fellowships (M.J.G.). We are also grateful to Dr. Alex Thom and Dr. David Pryde (Pfizer) for helpful discussions. The computational work was performed using the Darwin Supercomputer of the University of Cambridge High Performance Computing Service (<http://www.hpc.cam.ac.uk/>), provided by Dell, Inc., using Strategic Research Infrastructure Funding from the Higher Education Funding Council for England and funding from the Science and Technology Facilities Council. Mass spectrometry data were acquired at the EPSRC U.K. National Mass Spectrometry Facility at Swansea University.

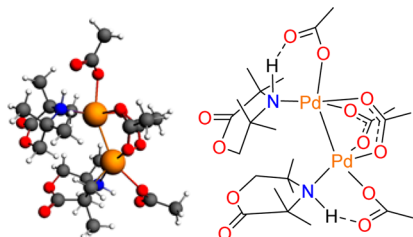
## ■ REFERENCES

- (1) (a) Jia, C.; Kitamura, T.; Fujiwara, Y. *Acc. Chem. Res.* **2001**, *34*, 633. (b) Godula, K.; Sames, D. *Science* **2006**, *312*, 67. (c) Davies, H. M. L.; Manning, J. R. *Nature* **2008**, *451*, 417. (d) Davies, H. M. L.; Du Bois, J.; Yu, J.-Q. *Chem. Soc. Rev.* **2011**, *40*, 1855. (e) Yamaguchi, J.; Yamaguchi, A. D.; Itami, K. *Angew. Chem., Int. Ed.* **2012**, *51*, 8960. (f) Mkhaliid, I. A. I.; Barnard, J. H.; Marder, T. B.; Murphy, J. M.; Hartwig, J. F. *Chem. Rev.* **2010**, *110*, 890.
- (2) (a) Dupont, J.; Consorti, C. S.; Spencer, J. *Chem. Rev.* **2005**, *105*, 2527. (b) Shilov, A. E.; Shul'pin, G. B. *Chem. Rev.* **1997**, *97*, 2879. (c) Neufeldt, S. R.; Sanford, M. S. *Acc. Chem. Res.* **2012**, *45*, 936.
- (3) (a) Desai, L. V.; Hull, K. L.; Sanford, M. S. *J. Am. Chem. Soc.* **2004**, *126*, 9542. (b) Zaitsev, V. G.; Shabashov, D.; Daugulis, O. *J. Am. Chem. Soc.* **2005**, *127*, 13154. (c) Giri, R.; Chen, X.; Yu, J.-Q. *Angew. Chem., Int. Ed.* **2005**, *44*, 2112. (d) Campeau, L.-C.; Schipper, D. J.; Fagnou, K. *J. Am. Chem. Soc.* **2008**, *130*, 3266. (e) Wang, D.-H.; Wasa, M.; Giri, R.; Yu, J.-Q. *J. Am. Chem. Soc.* **2008**, *130*, 7190.
- (4) (a) Giri, R.; Mauge, N.; Li, J.-J.; Wang, D.-H.; Breazzano, S. P.; Saunders, L. B.; Yu, J.-Q. *J. Am. Chem. Soc.* **2007**, *129*, 3510. (b) Simmons, E. M.; Hartwig, J. F. *Nature* **2012**, *483*, 70.
- (5) Ryabov, A. D.; Sakodinskaya, I. K.; Yatsimirsky, A. K. *J. Chem. Soc., Dalton Trans.* **1985**, 2629.
- (6) McNally, A.; Haffmayer, B.; Collins, B. S. L.; Gaunt, M. J. *Nature* **2014**, *510*, 129.
- (7) Giri, R.; Liang, J.; Lei, J.-G.; Li, J.-J.; Wang, D.-H.; Chen, X.; Naggar, I. C.; Guo, C.; Foxman, B. M.; Yu, J.-Q. *Angew. Chem., Int. Ed.* **2005**, *44*, 7420.
- (8) Ferretti, A. C.; Brennan, C.; Blackmond, D. G. *Inorg. Chim. Acta* **2011**, *369*, 292.
- (9) (a) Blackmond, D. G. *Angew. Chem., Int. Ed.* **2005**, *44*, 4302. (b) Baxter, R. D.; Sale, D.; Engle, K. M.; Yu, J.-Q.; Blackmond, D. G. *J. Am. Chem. Soc.* **2012**, *134*, 4600.
- (10) Jones, W. D.; Feher, F. *Acc. Chem. Res.* **1989**, *22*, 91.
- (11) Simmons, E. M.; Hartwig, J. F. *Angew. Chem., Int. Ed.* **2012**, *51*, 3066.
- (12) (a) Ryabov, A. D. *Chem. Rev.* **1990**, *90*, 403. (b) Davies, D. L.; Donald, S. M. A.; Macgregor, S. A. *J. Am. Chem. Soc.* **2005**, *127*, 13754.
- (13) (a) Cai, G.; Fu, Y.; Li, Y.; Wan, X.; Shi, Z. *J. Am. Chem. Soc.* **2007**, *129*, 7666. (b) Albrecht, M. *Chem. Rev.* **2010**, *110*, 576.
- (14) Hein, J. E.; Armstrong, A.; Blackmond, D. G. *Org. Lett.* **2011**, *13*, 4300.
- (15) Stephenson, T. A.; Morehouse, S. M.; Powell, A. R.; Heffer, J. P.; Wilkinson, G. *J. Chem. Soc.* **1965**, 3632.
- (16) Postulated Fujiwara-type intermediate:
 
- (17) Lu, W.; Jia, C.; Kitamura, T.; Fujiwara, Y. *Org. Lett.* **2000**, *2*, 2927.
- (18) (a) Nakata, K.; Yamaoka, Y.; Miyata, T.; Taniguchi, Y.; Takaki, K.; Fujiwara, Y. *J. Organomet. Chem.* **1994**, *473*, 329. (b) Fujiwara, Y.; Takaki, K.; Watanabe, J.; Uchida, Y.; Taniguchi, H. *Chem. Lett.* **1989**, 1687.
- (19) Explicit attempts to show that the main role of acetic anhydride was to dry the reaction were unsuccessful because addition of molecular sieves led to some decomposition of the starting material and MgSO<sub>4</sub> shut down the reaction.
- (20) Addition of 1 equiv of H<sub>2</sub>O was found to shut down the reaction, providing <5% product (Supporting Information).
- (21) Kerton, F. M.; Marriott, R. *Alternative Solvents for Green Chemistry*; RSC Publishing: Cambridge, U.K., 2013; pp 14–15.
- (22) Boutadla, Y.; Davies, D. L.; Macgregor, S. A.; Poblador-Bahamonde, A. I. *Dalton Trans.* **2009**, 5820.
- (23) (a) Te Velde, G.; Bickelhaupt, F. M.; Baerends, E. J.; Fonseca Guerra, C.; van Gisbergen, S. J. A.; Snijders, J. G.; Ziegler, T. *J. Comput. Chem.* **2001**, *22*, 931. (b) Fonseca Guerra, C.; Snijders, J. G.; te Velde, G.; Baerends, E. J. *Theor. Chem. Acc.* **1998**, *99*, 391. (c) *ADF2014*; SCM, Theoretical Chemistry, Vrije Universiteit, Amsterdam, The Netherlands, 2014. <http://www.scm.com>.
- (24) (a) Wassenaar, J.; Jansen, E.; van Zeist, W.-J.; Bickelhaupt, F. M.; Sieglar, M. A.; Spek, A. L.; Reek, J. N. H. *Nat. Chem.* **2010**, *2*, 417. (b) Wolters, L. P.; van Zeist, W.-J.; Bickelhaupt, F. M. *Chem. - Eur. J.* **2014**, *20*, 11370.
- (25) Lyngvi, E.; Sanhueza, I. A.; Schoenebeck, F. *Organometallics* **2015**, *34*, 805.
- (26) Species **4** is slightly higher in energy than the conformer formed through ring flip that places the palladium pseudoequatorial. However, the subsequent transition states for C–H cleavage were found to be substantially higher in energy (Supporting Information). Presumably, although the steric clash of the methyl groups of **4** results in a higher energy conformer, the resulting cyclopalladation is more favorable as a result of the C–H bonds being placed proximal to the metal center.
- (27) Melander, L. C. S.; Saunders, W. H. *Reaction Rates of Isotopic Molecules*; Wiley: New York, 1980; pp 44–45.
- (28) (a) Rousseaux, S.; Gorelsky, S. I.; Chung, B. K. W.; Fagnou, K. *J. Am. Chem. Soc.* **2010**, *132*, 10692. (b) García-Cuadrado, D.; Braga, A. A. C.; Maseras, F.; Echavarren, A. M. *J. Am. Chem. Soc.* **2006**, *128*, 1066. (c) Balcells, D.; Clot, E.; Eisenstein, O. *Chem. Rev.* **2010**, *110*, 749.
- (29) (a) Gorelsky, S. I.; Lapointe, D.; Fagnou, K. *J. Org. Chem.* **2012**, *77*, 658. (b) Usharani, D.; Lacy, D. C.; Borovik, A. S.; Shaik, S. *J. Am. Chem. Soc.* **2013**, *135*, 17090. (c) De Jong, G. T.; Bickelhaupt, F. M. *ChemPhysChem* **2007**, *8*, 1170. (d) Ess, D. H.; Houk, K. N. *J. Am. Chem. Soc.* **2008**, *130*, 10187. (e) Green, A. G.; Liu, P.; Merlic, C. A.; Houk, K. N. *J. Am. Chem. Soc.* **2014**, *136*, 4575.
- (30) Zhang, Q.; Yu, H.; Fu, Y. *Organometallics* **2013**, *32*, 4165.
- (31) (a) Hickman, A. J.; Sanford, M. S. *Nature* **2012**, *484*, 177. (b) Sehnal, P.; Taylor, R. J. K.; Fairlamb, I. J. S. *Chem. Rev.* **2010**, *110*, 824. (c) Dick, A. R.; Hull, K. L.; Sanford, M. S. *J. Am. Chem. Soc.* **2004**, *126*, 2300. (d) Yoneyama, T.; Crabtree, R. H. *J. Mol. Catal. A: Chem.* **1996**, *108*, 35. (e) Muñiz, K. *Angew. Chem., Int. Ed.* **2009**, *48*, 9412. (f) Cheng, X.-F.; Li, Y.; Su, Y.-M.; Yin, F.; Wang, J.-Y.; Sheng, J.; Vora, H. U.; Wang, X.-S.; Yu, J.-Q. *J. Am. Chem. Soc.* **2013**, *135*, 1236.

(32) Camasso, N. M.; Pérez-Temprano, M. H.; Sanford, M. S. *J. Am. Chem. Soc.* **2014**, *136*, 12771.

(33) Powers, D. C.; Ritter, T. *Nat. Chem.* **2009**, *1*, 302.

(34) Possible palladium(III) bimetallic intermediate:



$\text{Pd(II) (10) + Pd(IV) (11) \rightarrow Pd(III)}$ ;  $\Delta G = + 8.4 \text{ kcal mol}^{-1}$

(35) Intermediate **18** is  $-39.7 \text{ kcal mol}^{-1}$  lower in energy than intermediate **10**. Therefore, all species in [Figure 12](#) are not kinetically relevant as expected from the experimental data.

(36) Changing the position of the acetate ligands on the palladium(IV) species gave higher energy intermediates ([Supporting Information](#)). Also, note that the bidentate acetate trans to the substrate does not stop the C–N reductive elimination (to give  $\text{TS}^\ddagger \mathbf{3}$ ) from being symmetry-allowed<sup>38</sup> because during the reaction the acetate binding changes from a  $\kappa^2$  to a  $\kappa^{-1}$  coordination mode.

(37) (a) Nardes, E. T.; Daugulis, O. *J. Am. Chem. Soc.* **2012**, *134*, 7. (b) He, G.; Zhao, Y.; Zhang, S.; Lu, C.; Chen, G. *J. Am. Chem. Soc.* **2012**, *134*, 3. (c) Wang, C.; Chen, C.; Zhang, J.; Han, J.; Wang, Q.; Guo, K.; Liu, P.; Guan, M.; Yao, Y.; Zhao, Y. *Angew. Chem., Int. Ed.* **2014**, *53*, 9884.

(38) Braterman, P. S. *J. Chem. Soc., Chem. Commun.* **1979**, 70–71.